Feasible Safe Connected Cruise Control with Backstepping Control Barrier Functions

Yuchen Chen, Tamas G. Molnar, and Gábor Orosz

***Abstract*— This paper proposes a safety-critical connected cruise control strategy using backstepping control barrier functions to enforce safety for connected automated vehicles while satisfying actuator limits. The proposed approach accounts for the vehicle's response time, modeled as a first-order lag. We investigate the impact of braking limits and lag time on the conservativeness of the safe region in the state space. Using simulations, we confirm that the proposed controller ensures safety while maintaining feasibility.**

I. Introduction

Vehicle-to-everything (V2X) communication enhances the capabilities of connected automated vehicles (CAVs) by improving safety, energy efficiency, and driving comfort. Connectivity allows CAVs to exchange information with other road participants, enabling the design of more advanced on-board controllers. Well-designed controllers have been proven to improve energy efficiency [1], and alleviate traffic congestion [2], [3].

The most crucial requirement for CAV control is safety. This can be guaranteed using different approaches, including reachability analysis [4], reinforcement learning [5], and model predictive control [6]. Recently, control barrier functions (CBFs) [7] have gained traction due to their adaptability to existing control frameworks and low computational cost. Existing studies have utilized CBFs to address various challenges: high-order dynamics using high-order CBFs [8], [9] and backstepping CBFs [10], time delays [11], and input constraints [12]. Safe connected cruise control (CCC) was first developed using CBFs in [13], with detailed analyses in [14], [15]. A recent extension of safe CCC incorporating vehicle response lag was proposed in [16] using high-order CBFs [9]. However, these methods neglect input constraints, potentially leading to infeasibly large control efforts for safety assurance.

In this paper, we design a safe CCC strategy that explicitly incorporates input constraints and ensures longitudinal safety for CAVs, while accounting for vehicle response time modeled as a first-order lag. To achieve this, we use backstepping CBFs to construct safety-critical CCC laws that maintain performance while enforcing safety with minimal modifications to existing, potentially unsafe control designs.

Y. Chen is with the Department of Mechanical Engineering, University of Michigan, Ann Arbor, MI 48109, USA, ethanch@umich.edu.

G. Orosz is with the Department of Mechanical Engineering and with the Department of Civil and Environmental Engineering, University of Michigan, Ann Arbor, MI 48109, USA, orosz@umich.edu.

T. G. Molnar is with the Department of Mechanical Engineering, Wichita State University, Wichita, KS 67260, USA, tamas.molnar@wichita.edu.

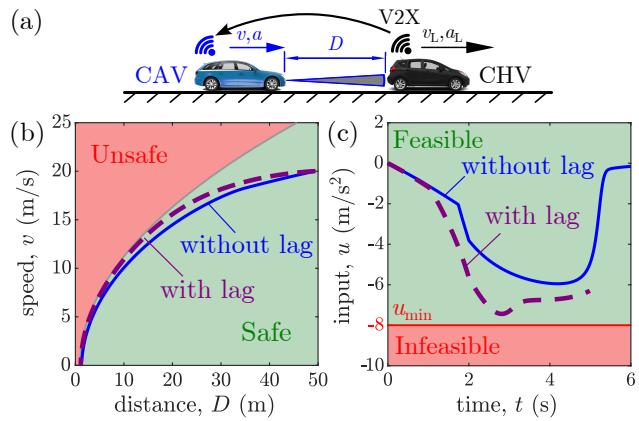

Fig. 1. (a) A connected automated vehicle (CAV) follows a preceding connected human-driven vehicle (CHV) using vehicle-to-everything (V2X) connectivity. The proposed safety-critical connected cruise controller (CCC) can (b) guarantee safety while (c) satisfying control input constraints, both without ($\xi = 0\,\mathrm{s}$) and with first-order lag ($\xi = 0.8\,\mathrm{s}$).

The proposed controllers are guaranteed to satisfy actuator limits through appropriate tuning of backstepping CBFs. We analyze how braking capacity and first-order lag influence the conservativeness of the proposed controllers. Our simulations demonstrate the performance of these controllers, showing safety guarantees with feasibility; see Fig. 1.

The rest of the paper is structured as follows. Section II introduces the CAV dynamics. Section III revisits CBF theory, including backstepping CBFs. Section IV proposes a novel safety-critical CCC for CAVs without and with first-order lag, and describes the simulations. Section V concludes the results and points out future directions.

II. Connected Cruise Control

Consider the scenario in Fig. 1(a), where a connected automated vehicle (CAV) follows a preceding connected human-driven vehicle (CHV). The CAV measures its own speed $v \geq 0$, acceleration a, and distance D using on-board sensors. Additionally, it can also obtain the CHV's velocity $v_\mathrm{L} \geq 0$ and acceleration a_L via V2X communication.

We represent the CAV's dynamics by two models with different fidelity. First, we utilize a double integrator model:

$$\begin{aligned} \dot{D} &= v_\mathrm{L} - v, \\ \dot{v} &= u, \end{aligned} \tag{1}$$

with state $\mathbf{x} = \begin{bmatrix} D & v \end{bmatrix}^\top$ and control input u. Since the powertrain dynamics and V2X communication may introduce time delays [7], [17], we also adopt a more descriptive model that incorporates the CAV's response time as a first-order lag

$\xi > 0$:

$$\begin{aligned} \dot{D} &= v_{\mathrm{L}} - v, \\ \dot{v} &= a, \\ \dot{a} &= \frac{1}{\xi}(u - a), \end{aligned} \tag{2}$$

with state $\mathbf{x} = \begin{bmatrix} D & v & a \end{bmatrix}^\top$. For simplicity, we omit rolling resistance and air drag in both models, which could potentially reduce speed and improve safety.

Given these models, this paper aims to design a CAV controller that ensures safety while satisfying the input limits $u_{\min} \leq u \leq u_{\max}$. We choose the connected cruise control (CCC) strategy [18] as the desired controller $u = k_{\mathrm{d}}(\mathbf{x})$:

$$k_{\mathrm{d}}(\mathbf{x}) = \mathrm{sat}\Big(A\big(V(D) - v\big) + B\big(W(v_{\mathrm{L}}) - v\big)\Big). \tag{3}$$

Here the CAV responds to the distance and the velocity difference using gains $A, B \geq 0$, respectively. The saturation function

$$\mathrm{sat}(u) = \max\left\{u_{\min}, \min\{u, u_{\max}\}\right\}, \tag{4}$$

encodes the input constraints. The range policy

$$V(D) = \max\left\{0, \min\{\kappa(D - D_{\mathrm{st}}), v_{\max}\}\right\}, \tag{5}$$

sets the desired speed based on the distance D, starting at zero at D_{st} and increasing linearly with slope κ until the speed limit $v_{\max}$ is reached. The speed policy

$$W(v_{\mathrm{L}}) = \min\{v_{\mathrm{L}}, v_{\max}\}, \tag{6}$$

is used to avoid following a leader who exceeds $v_{\max}$.

While the desired controller (3) has shown good performance in car-following experiments [17], it may only guarantee safety for a restricted selection of gains [15]. Here, we utilize control barrier functions to minimally modify the desired controller $u = k_{\mathrm{d}}(\mathbf{x})$ in (3) and synthesize a safe controller $u = k(\mathbf{x})$ that still satisfies $u_{\min} \leq u \leq u_{\max}$.

III. Backstepping Control Barrier Functions

In this section, we first review the theory of control barrier functions (CBFs), then introduce backstepping CBFs.

Consider a control-affine system:

$$\dot{\mathbf{x}} = \mathbf{f}(\mathbf{x}) + \mathbf{g}(\mathbf{x})\mathbf{u}, \tag{7}$$

with state $\mathbf{x} \in \mathbb{R}^n$, input $\mathbf{u} \in \mathbb{R}^m$, and dynamics given by the locally Lipschitz continuous functions $\mathbf{f} : \mathbb{R}^n \to \mathbb{R}^n$ and $\mathbf{g} : \mathbb{R}^n \to \mathbb{R}^{n\times m}$. Given a locally Lipschitz continuous controller $\mathbf{k} : \mathbb{R}^n \to \mathbb{R}^m$, $\mathbf{u} = \mathbf{k}(\mathbf{x})$, we have the closed-loop system:

$$\dot{\mathbf{x}} = \mathbf{f}(\mathbf{x}) + \mathbf{g}(\mathbf{x})\mathbf{k}(\mathbf{x}), \tag{8}$$

that has the solution $\mathbf{x}(t)$ for an initial condition $\mathbf{x}(0) \in \mathbb{R}^n$. To evaluate the safety of (8), we define a continuously differentiable function $h : \mathbb{R}^n \to \mathbb{R}$ and a corresponding safe set:

$$\mathcal{S} = \left\{\mathbf{x} \in \mathbb{R}^n : h(\mathbf{x}) \geq 0\right\}. \tag{9}$$

System (8) is safe w.r.t. $\mathcal{S}$ if $\mathbf{x}(t) \in \mathcal{S}$ holds for all time for any $\mathbf{x}(0) \in \mathcal{S}$. Nagumo's theorem [19] establishes safety.

Theorem 1 ([19]). *Let h satisfy $\nabla h(\mathbf{x}) \neq \mathbf{0}$ for all $\mathbf{x} \in \mathbb{R}^n$ such that $h(\mathbf{x}) = 0$. System (8) is safe w.r.t. $\mathcal{S}$ if and only if:*

$$\dot{h}\big(\mathbf{x}, \mathbf{k}(\mathbf{x})\big) \geq 0, \quad \forall \mathbf{x} \in \mathbb{R}^n \text{ s.t. } h(\mathbf{x}) = 0, \tag{10}$$

where

$$\dot{h}\big(\mathbf{x}, \mathbf{k}(\mathbf{x})\big) = \underbrace{\nabla h(\mathbf{x})\mathbf{f}(\mathbf{x})}_{L_{\mathbf{f}}h(\mathbf{x})} + \underbrace{\nabla h(\mathbf{x})\mathbf{g}(\mathbf{x})}_{L_{\mathbf{g}}h(\mathbf{x})}\mathbf{k}(\mathbf{x}). \tag{11}$$

To synthesize safety-critical controllers for (7), control barrier functions (CBFs) [20] have been proposed.

Definition 1 ([20]). Function h is a control barrier function for (7) on $\mathcal{S}$ if there exists $\alpha \in \mathcal{K}^{\mathrm{e}}$ such that for all $x \in \mathcal{S}$:

$$\sup_{\mathbf{u}\in\mathbb{R}^m} \dot{h}(\mathbf{x}, \mathbf{u}) > -\alpha\big(h(\mathbf{x})\big). \tag{12}$$

Remark 1. A continuous function $\alpha : \mathbb{R} \to \mathbb{R}$ is of extended class-$\mathcal{K}$ ($\alpha \in \mathcal{K}^{\mathrm{e}}$) if it is strictly increasing and $\alpha(0) = 0$.

Theorem 2 ([20]). *If h is a CBF for (7) on $\mathcal{S}$, then any locally Lipschitz continuous controller $\mathbf{k}(\mathbf{x})$ that satisfies:*

$$\dot{h}\big(\mathbf{x}, \mathbf{k}(\mathbf{x})\big) \geq -\alpha\big(h(\mathbf{x})\big), \tag{13}$$

for all $\mathbf{x} \in \mathcal{S}$ renders (8) safe w.r.t. $\mathcal{S}$.

Condition (13) can be used as a constraint in optimization to synthesize safe controllers. For example, given a desired but not necessarily safe controller $\mathbf{k}_{\mathrm{d}} : \mathbb{R}^n \to \mathbb{R}^m$, we can design a so-called safety filter that minimally modifies $\mathbf{k}_{\mathrm{d}}(\mathbf{x})$ subject to (13):

$$\begin{aligned} \mathbf{k}(\mathbf{x}) = \underset{\mathbf{u}\in\mathbb{R}^m}{\operatorname{argmin}} \quad & \|\mathbf{u} - \mathbf{k}_{\mathrm{d}}(\mathbf{x})\|^2 \\ \text{s.t.} \quad & \dot{h}(\mathbf{x}, \mathbf{u}) \geq -\alpha\big(h(\mathbf{x})\big). \end{aligned} \tag{14}$$

Remark 2. The strict inequality in (12) ensures the Lipschitz continuity of optimization-based controllers like (14) at points where $L_{\mathbf{g}}h(\mathbf{x}) = \mathbf{0}$ [21]. One may relax (12) to nonstrict inequality as in (13) for other controllers that are Lipschitz continuous.

For scalar input u, as in (1), (2), the solution of (14) is

$$k(\mathbf{x}) = \begin{cases} \min\left\{k_{\mathrm{d}}(\mathbf{x}), k_{\mathrm{s}}(\mathbf{x})\right\}, & \text{if } L_{\mathbf{g}}h(\mathbf{x}) < 0, \\ k_{\mathrm{d}}(\mathbf{x}), & \text{if } L_{\mathbf{g}}h(\mathbf{x}) = 0, \\ \max\left\{k_{\mathrm{d}}(\mathbf{x}), k_{\mathrm{s}}(\mathbf{x})\right\}, & \text{if } L_{\mathbf{g}}h(\mathbf{x}) > 0, \end{cases} \tag{15}$$

with

$$k_{\mathrm{s}}(\mathbf{x}) = -\frac{L_{\mathbf{f}}h(\mathbf{x}) + \alpha\big(h(\mathbf{x})\big)}{L_{\mathbf{g}}h(\mathbf{x})}, \tag{16}$$

see [7]. Note that when $L_{\mathbf{g}}h(\mathbf{x}) \equiv \mathbf{0}$ for all $\mathbf{x} \in \mathcal{S}$, the input $\mathbf{u}$ does not directly affect the safety of (8) based on (11). Therefore, h is neither a valid CBF nor applicable to synthesize safety-critical controllers.

A common approach to address this issue is to construct a CBF candidate known as a high-order CBF [8], [9]. However, proving its validity as a CBF can be challenging [22], [23], and safe CCC designs based on high-order CBFs may suffer from feasibility issues [16]. As an alternative, backstepping CBFs have been proposed to ensure valid CBF construc-

tion [10], [24]. In the following sections, we will demonstrate that safe CCC using backstepping CBFs preserves feasibility. To this end, we first assume that system (7) is an r-layer cascaded system in strict feedback form:

$$\begin{bmatrix}\dot{\mathbf{x}}_1\\ \dot{\mathbf{x}}_2\\ \vdots\\ \dot{\mathbf{x}}_r\end{bmatrix}=\begin{bmatrix}\mathbf{f}_1(\mathbf{x}_1)+\mathbf{g}_1(\mathbf{x}_1)\mathbf{x}_2\\ \mathbf{f}_2(\mathbf{x}_1,\mathbf{x}_2)+\mathbf{g}_2(\mathbf{x}_1,\mathbf{x}_2)\mathbf{x}_3\\ \vdots\\ \mathbf{f}_r(\mathbf{x})\end{bmatrix}+\begin{bmatrix}\mathbf{0}\\ \mathbf{0}\\ \vdots\\ \mathbf{g}_r(\mathbf{x})\end{bmatrix}\mathbf{u}, \quad (17)$$

with $\mathbf{x}_1\in\mathbb{R}^{n_1},\mathbf{x}_2\in\mathbb{R}^{n_2},\dots,\mathbf{x}_r\in\mathbb{R}^{n_r}$ and $\sum_{j=1}^{r}n_j=n$. Then, by considering the top i layers $i\in\{1,\cdots,r-1\}$ and viewing $\mathbf{u}_i=\mathbf{x}_{i+1}$ as a virtual control input, we can define the corresponding reduced-order models (ROMs):

$$\dot{\mathbf{z}}_i=\mathbf{F}_i(\mathbf{z}_i)+\mathbf{G}_i(\mathbf{z}_i)\mathbf{u}_i, \quad (18)$$

with $\mathbf{z}_i=\left[\mathbf{x}_1^\top,\cdots,\mathbf{x}_i^\top\right]^\top\in\mathbb{R}^{q_i}$, $q_i=\sum_{j=1}^{i}n_j$ and:

$$\mathbf{F}_i(\mathbf{z}_i)=\begin{bmatrix}\mathbf{f}_1(\mathbf{x}_1)+\mathbf{g}_1(\mathbf{x}_1)\mathbf{x}_2\\ \vdots\\ \mathbf{f}_i(\mathbf{z}_i)\end{bmatrix},\ \mathbf{G}_i(\mathbf{z}_i)=\begin{bmatrix}\mathbf{0}\\ \vdots\\ \mathbf{g}_i(\mathbf{z}_i)\end{bmatrix}. \quad (19)$$

If $h(\mathbf{x}_1)$ is a CBF for $\dot{\mathbf{x}}_1=\mathbf{f}_1(\mathbf{x}_1)+\mathbf{g}_1(\mathbf{x}_1)\mathbf{x}_2$ with the corresponding safe set $\mathcal{S}_1$, and the right pseudo-inverse of $\mathbf{g}_i(\mathbf{z}_i)$ exist for all $i\in\{2,\cdots,r\}$ in (17), then backstepping provides a method to construct a sequence of valid CBFs for (18) from $h_1(\mathbf{z}_1)=h(\mathbf{x}_1)$ [10], [24]:

$$h_{i+1}(\mathbf{z}_{i+1})=h_i(\mathbf{z}_i)-\frac{1}{2\mu_i}\left\|\mathbf{x}_{i+1}-\mathbf{k}_i(\mathbf{z}_i)\right\|^2, \quad (20)$$

for $i\in\{1,...,r-1\}$ with corresponding safe sets:

$$\mathcal{S}_{i+1}=\{\mathbf{x}\in\mathbb{R}^n: h_{i+1}(\mathbf{z}_{i+1})\geq 0\}. \quad (21)$$

In (20), $\mu_i>0$ are backstepping CBF parameters and $\mathbf{k}_i:\mathbb{R}^{q_i}\to\mathbb{R}^{n_{i+1}}$ are smooth safe controllers that satisfy:

$$L_{\mathbf{F}_i}h_i(\mathbf{z}_i)+L_{\mathbf{G}_i}h_i(\mathbf{z}_i)\mathbf{k}_i(\mathbf{z}_i)>-\alpha_i\big(h_i(\mathbf{z}_i)\big), \quad (22)$$

for all $\mathbf{z}_i$ such that $\mathbf{x}\in\mathcal{S}_i$, cf. (12), with $\alpha_i\in\mathcal{K}^{\mathrm{e}}$ such that $\alpha_{i+1}(s)\geq\alpha_i(s)$ for all $s\in\mathbb{R}$.

Theorem 3 ([24]). *Let h_r be the CBF defined by (20) with $\alpha_r\in\mathcal{K}^{\mathrm{e}}$. Then, any locally Lipschitz continuous controller $\mathbf{k}(\mathbf{x})$ that satisfies:*

$$\dot{h}_r\big(\mathbf{x},\mathbf{k}(\mathbf{x})\big)\geq-\alpha_r\big(h_r(\mathbf{x})\big), \quad (23)$$

for all $\mathbf{x}\in\mathcal{S}_r$ renders (8) safe w.r.t. $\mathcal{S}_r\subset\mathcal{S}_1$.

Similar to (14), (23) can also construct the safety filter:

$$\begin{aligned}\mathbf{k}(\mathbf{x})=\underset{\mathbf{u}\in\mathbb{R}^m}{\operatorname{argmin}}\quad&\|\mathbf{u}-\mathbf{k}_{\mathrm{d}}(\mathbf{x})\|^2\\ \text{s.t.}\quad&\dot{h}_r\big(\mathbf{x},\mathbf{u}\big)\geq-\alpha_r\big(h_r(\mathbf{x})\big).\end{aligned} \quad (24)$$

The solution of (24) for a scalar input u matches (15), (16), with h and α replaced by h_r and α_r.

Remark 3. Similar to (12), the strict inequality in (22) guarantees the Lipschitz continuity of controllers synthesized by (20) when $L_{\mathbf{G}_i}h_i(\mathbf{z}_i)=\mathbf{0}$ [24]. Here, we adopt the nonstrict inequality in (22).

IV. Feasible Safe Connected Cruise Control

In this section, we first introduce the backstepping CBF for the CAV dynamics without lag (1), and propose the corresponding feasible safety-critical CCC law via Theorem 3. Then, we extend this approach to incorporate the first-order lag in (2) and derive the associated safety-critical CCC.

A. Safety without First-order Lag

Now, we compute the backstepping CBF based on (20) for the lag-free model (1). First, we rewrite the system (1) in the form of (17):

$$\underbrace{\begin{bmatrix}\dot{D}\\ \dot{v}\end{bmatrix}}_{\dot{\mathbf{x}}}=\underbrace{\begin{bmatrix}v_{\mathrm{L}}-v\\ 0\end{bmatrix}}_{\mathbf{f}(\mathbf{x})}+\underbrace{\begin{bmatrix}0\\ 1\end{bmatrix}}_{\mathbf{g}(\mathbf{x})}u, \quad (25)$$

and select the first row in (25) as the ROM:

$$\underbrace{\dot{D}}_{\dot{\mathbf{z}}_1}=\underbrace{v_{\mathrm{L}}}_{\mathbf{F}_1(\mathbf{z}_1)}+\underbrace{(-1)}_{\mathbf{G}_1(\mathbf{z}_1)}v. \quad (26)$$

cf. (18), (19). Then we choose the function h_1 to quantify the safety of the CAV. A simple idea is to keep the CAV's distance from the CHV above a safe distance $D_{\mathrm{sf}}>0$ to avoid collision:

$$h_1(\mathbf{z}_1)=D-D_{\mathrm{sf}}, \quad (27)$$

with the set $\mathcal{S}_1=\{\mathbf{x}\in\mathbb{R}^2: h_1(\mathbf{z}_1)\geq 0\}$. As $L_{\mathbf{G}_1}h_1(\mathbf{z}_1)\equiv-1$ and $L_{\mathbf{g}}h_1(\mathbf{x})\equiv 0$ for all $\mathbf{x}\in\mathcal{S}$, h_1 is a CBF for the ROM (26) but not for the full-order dynamics (25). Therefore, we construct a backstepping CBF for (25) from h_1 in (27) based on (20). In (26), v is the virtual control input, which should be selected as the safe velocity $v=k_1(\mathbf{z}_1)$ that satisfies (22):

$$v_{\mathrm{L}}-k_1(\mathbf{z}_1)\geq-\alpha_1(D-D_{\mathrm{sf}}). \quad (28)$$

Since $v_{\mathrm{L}}\geq 0$ and $-\alpha_1(D-D_{\mathrm{sf}})\leq 0$ for all $\mathbf{x}\in\mathcal{S}$, we choose $k_1(\mathbf{z}_1)\equiv 0$ and construct the backstepping CBF (20):

$$h_2(\mathbf{x})=h_1(\mathbf{z}_1)-\frac{\big(v-k_1(\mathbf{z}_1)\big)^2}{2\mu_1}=D-D_{\mathrm{sf}}-\frac{v^2}{2\mu_1}, \quad (29)$$

with $\mu_1>0$ and $\mathcal{S}_2=\{\mathbf{x}\in\mathbb{R}^2: h_2(\mathbf{x})\geq 0\}$.

Fig. 2 illustrates the sets $\mathcal{S}_1$ (red) and $\mathcal{S}_2$ (blue), defined by (27) and (29), in both the (D,v,a) and (D,v) spaces. Note that the additional state a (CAV acceleration) is included in Fig. 2(a) solely for comparison with Fig. 4 shown below, while the CBF in (29) does not depend on a. Importantly, we observe that when system (25) travels along the safe boundary (blue), it applies constant acceleration input $u=-\mu_1$. Note that $\mathcal{S}_2\subset\mathcal{S}_1$, and $\mathcal{S}_2$ expands with increasing μ_1, approaching $\mathcal{S}_1$ as $\mu_1\to\infty$; see Fig. 2(b).

Next, we can establish safety-critical CCC based on Theorem 3 by using the safety filter (24) and choosing CCC (3) as desired controller k_{d}. For h_2 in (29), we have $\nabla h_2(\mathbf{x})=\begin{bmatrix}1 & -v/\mu_1\end{bmatrix}$, $L_{\mathbf{f}}h_2(\mathbf{x})=v_{\mathrm{L}}-v$ and $L_{\mathbf{g}}h_2(\mathbf{x})=-v/\mu_1$, thus the safety filter (15) becomes:

$$k_2(\mathbf{x})=\begin{cases}\min\left\{k_{\mathrm{d}}(\mathbf{x}),k_2^{\mathrm{s}}(\mathbf{x})\right\}, & \text{if } v>0,\\ k_{\mathrm{d}}(\mathbf{x}), & \text{if } v=0.\end{cases} \quad (30)$$

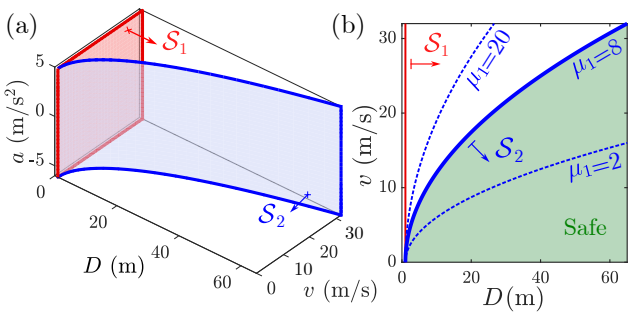

Fig. 2. Safe sets $\mathcal{S}_1$ and $\mathcal{S}_2$, defined by the safe distance h_1 in (27), and the backstepping CBF h_2 in (29), respectively, for various μ_1 values (with unit m/s^2) in (b). Arrows indicate the safe side of the set boundaries.

TABLE I

PARAMETERS OF THE SIMULATIONS

Vehicle	Variable	Symbol	Value	Unit
CAV	acceleration limit	$(u_{\min}, u_{\max})$	$(-8, 3)$	m/s^2
	speed limit	$v_{\max}$	25	m/s
	standstill distance	D_{st}	5	m
	range policy gradient	κ	0.6	1/s
	CCC gains	(A, B)	$(0.1, 0.1)$	1/s
	safe distance	D_{sf}	1	m
	CBF parameter (no lag)	μ_1	8	m/s^2
	CBF parameters (lag)	(μ_1, μ_2)	$(6, 0.8)$	m/s^2, m/s^4
	class-$\mathcal{K}$ function	γ	1	1/s
CHV	deceleration	a_{dec}	-10	m/s^2

while (16) reads:

$$k_2^{\text{s}}(\mathbf{x}) = \frac{\mu_1}{v}\left(v_{\text{L}} - v + \alpha_2\left(D - D_{\text{sf}} - \frac{v^2}{2\mu_1}\right)\right), \tag{31}$$

where we choose $\alpha_2(s) = \gamma s$ with $\gamma > 0$.

Although $k_2^{\text{s}}(\mathbf{x})$ in (31) has a singularity at $v = 0$, k_2 (30) avoids it as $k_2(\mathbf{x}) = k_{\text{d}}(\mathbf{x})$ when $v = 0$, and $k_{\text{d}}(\mathbf{x})$ in (3) is well-defined. Furthermore, the value of $k_2(\mathbf{x})$ can be bounded, as shown in the following theorem.

Theorem 4. *Controller (30), (31) satisfies the input constraint $u_{\min} \le u \le u_{\max}$ for all $\mathbf{x} \in \mathcal{S}_2$ if:*

$$u_{\min} \le -\mu_1. \tag{32}$$

Proof. First, considering the case $v = 0$ in (30), we have $k_2(\mathbf{x}) = k_{\text{d}}(\mathbf{x}) \in [u_{\min}, u_{\max}]$ based on (3), (4).

Next, for $v > 0$, $k_2(\mathbf{x}) = \min\{k_{\text{d}}(\mathbf{x}), k_2^{\text{s}}(\mathbf{x})\}$. In this case, $k_2(\mathbf{x}) \le k_{\text{d}}(\mathbf{x}) \le u_{\max}$. Furthermore, since $\mu_1 > 0$, $v_{\text{L}} \ge 0$, and $\alpha_2\left(D - D_{\text{sf}} - \frac{v^2}{2\mu_1}\right) \ge 0$ for all $\mathbf{x} \in \mathcal{S}_2$, $k_2^{\text{s}}(\mathbf{x})$ in (31) satisfies:

$$k_2^{\text{s}}(\mathbf{x}) \ge -\mu_1 \ge u_{\min}. \tag{33}$$

Thus, $k_2^{\text{s}}(\mathbf{x}) \ge u_{\min}$ and $k_{\text{d}}(\mathbf{x}) \ge u_{\min}$ both hold, which implies $k_2(\mathbf{x}) \in [u_{\min}, u_{\max}]$, and Theorem 4 holds. □

Theorem 4 indicates that the safety filter (30), (31) meets the input constraints if parameter μ_1 satisfies (32).

To evaluate the proposed controllers, we simulate a car-following scenario shown in Fig. 1(a), using safety-critical CCC with backstepping CBF (3), (30), (31) for system (1). The results are illustrated in Fig. 3 using the parameters in Table I. Note that we selected relatively small CCC gains A and B_1 to better illustrate the safety filter engagements.

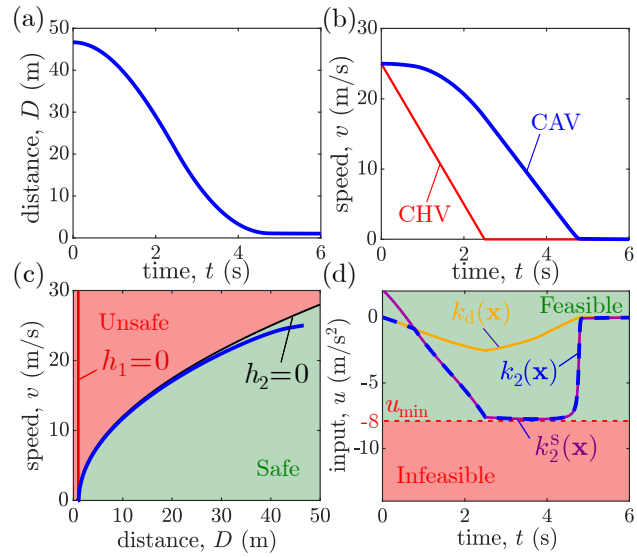

Fig. 3. Simulations of the car-following system without lag (1) using the safety filter with backstepping CBF (3), (30), (31).

The simulation depicts a CHV performing emergency braking with constant deceleration a_{dec} until it comes to a halt; see Fig. 3(b). Using the safety-critical CCC, the CAV responds to the CHV by decelerating and finally stopping within the safe distance; see Fig. 3(a). Accordingly, in panel (c), the state trajectory (blue) always stays inside the safe set, indicating that the safety filter prevents safety violations. Importantly, by selecting $\mu_1 = -u_{\min}$, the backstepping CBF ensures provable safety guarantees while satisfying actuator limits; see the safety filter input $k_2(\mathbf{x}) > u_{\min}$ (blue) in Fig. 3(d). Moreover, unlike the safety-critical CCC based on the high-order CBF (time to conflict criterion) in [14], $k_2^{\text{s}}(\mathbf{x})$ in (31) is independent of the CHV's acceleration a_{L}. This reduces sensitivity to the CHV's motion and improves comfort by reducing jerk during deceleration. The cost for these benefits is a more conservative safe set; see Fig. 2.

B. Safety with First-order Lag

Now, we incorporate a first-order lag into the CAV's dynamics as in (2), derive the backstepping CBF based on (20), (29), and show that the corresponding safety filter still satisfies input constraints when properly choosing the CBF parameters. First, we rewrite system (2) in the form of (17):

$$\underbrace{\begin{bmatrix} \dot{D} \\ \dot{v} \\ \dot{a} \end{bmatrix}}_{\dot{\mathbf{x}}} = \underbrace{\begin{bmatrix} v_{\text{L}} - v \\ a \\ -\frac{1}{\xi}a \end{bmatrix}}_{\mathbf{f}(\mathbf{x})} + \underbrace{\begin{bmatrix} 0 \\ 0 \\ \frac{1}{\xi} \end{bmatrix}}_{\mathbf{g}(\mathbf{x})} u. \tag{34}$$

From Section IV.A, h_2 in (29) is a CBF for the ROM:

$$\underbrace{\begin{bmatrix} \dot{D} \\ \dot{v} \end{bmatrix}}_{\dot{\mathbf{z}}_2} = \underbrace{\begin{bmatrix} v_{\text{L}} - v \\ 0 \end{bmatrix}}_{\mathbf{F}_2(\mathbf{z}_2)} + \underbrace{\begin{bmatrix} 0 \\ 1 \end{bmatrix}}_{\mathbf{G}_2(\mathbf{z}_2)} a, \tag{35}$$

and $L_{\mathbf{g}} h_2(\mathbf{x}) \equiv 0$ for all $\mathbf{x} \in \mathbb{R}^3$. Therefore, one may backstep one more time to obtain a backstepping CBF for (34).

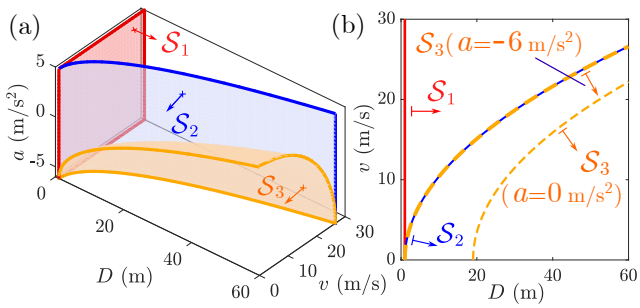

Fig. 4. Safe sets $\mathcal{S}_1$, $\mathcal{S}_2$, and $\mathcal{S}_3$, defined by the safe distance h_1 in (27), the backstepping CBF h_2 in (29) for the CAV without lag (1), and the backstepping CBF h_3 in (37) with lag (2), respectively. Arrows indicate the safe side of the set boundaries.

To achieve that, the virtual input a in (35) is selected as the safe acceleration $a = k_2(\mathbf{z}_2)$ satisfying (22) for $i = 2$:

$$v_{\mathrm{L}} - v - \frac{v k_2(\mathbf{z}_2)}{\mu_1} \geq -\alpha_2\Big(D - D_{\mathrm{sf}} - \frac{v^2}{2\mu_1}\Big). \tag{36}$$

Note that instead of using the non-smooth but safe controller k_2 in (30) as the safe acceleration, we adopt a simpler alternative $k_2(\mathbf{z}_2) \equiv -\mu_1$, which satisfies (36) since $v_{\mathrm{L}} \geq 0$ and $-\alpha_2(D - D_{\mathrm{sf}} - \frac{v^2}{2\mu_1}) \leq 0$ for all $\mathbf{x} \in \mathcal{S}_1$. We then establish the backstepping CBF as in (20):

$$h_3(\mathbf{x}) = h_2(\mathbf{z}_2) - \frac{\big(a - k_2(\mathbf{z}_2)\big)^2}{2\mu_2} = D - D_{\mathrm{sf}} - \frac{v^2}{2\mu_1} - \frac{(a+\mu_1)^2}{2\mu_2}, \tag{37}$$

with $\mu_1, \mu_2 > 0$ and $\mathcal{S}_3 = \{\mathbf{x} \in \mathbb{R}^3 : h_3(\mathbf{x}) \geq 0\}$.

Fig. 4 visualizes the sets $\mathcal{S}_1$, $\mathcal{S}_2$, and $\mathcal{S}_3$ given by (27), (29), and (37), in the (D, v, a) and (D, v) spaces, with red, blue, and yellow color, respectively. Note that $\mathcal{S}_3 \subset \mathcal{S}_2 \subset \mathcal{S}_1$, and $\mathcal{S}_3$ (yellow) approaches $\mathcal{S}_2$ (blue) as $\mu_2 \to \infty$.

As Theorem 3 applies to h_3, we can consider CCC (3) as nominal controller k_{d} and use the safety filter (15):

$$k_3(\mathbf{x}) = \begin{cases} \min\{k_{\mathrm{d}}(\mathbf{x}), k_3^{\mathrm{s}}(\mathbf{x})\}, & \text{if } a > -\mu_1, \\ k_{\mathrm{d}}(\mathbf{x}), & \text{if } a = -\mu_1, \\ \max\{k_{\mathrm{d}}(\mathbf{x}), k_3^{\mathrm{s}}(\mathbf{x})\}, & \text{if } a < -\mu_1, \end{cases} \tag{38}$$

where (16) gives:

$$k_3^{\mathrm{s}}(\mathbf{x}) = a + \frac{\mu_2 \xi}{a + \mu_1}\Big(v_L - v - \frac{va}{\mu_1} + \alpha_3\big(h_3(\mathbf{x})\big)\Big), \tag{39}$$

and we still choose $\alpha_3(s) = \gamma s$ with $\gamma > 0$.

Controller (38) avoids the singularity at $a = -\mu_1$, since $k_3(\mathbf{x}) = k_{\mathrm{d}}(\mathbf{x})$ when $a = -\mu_1$, and $k_{\mathrm{d}}(\mathbf{x})$ is well-defined. Moreover, we will show that the value of $k_3(\mathbf{x})$ can also be bounded under some assumptions in the following theorem.

Theorem 5. *Let $v \in [0, v_{\max}]$ hold with some maximum velocity $v_{\max} > 0$ for the CAV. Controller (38), (39) satisfies the input constraint $u_{\min} \leq u \leq u_{\max}$ for all $\mathbf{x} \in \mathcal{S}_3$ if:*

$$u_{\max} \geq -\mu_1 \quad \text{and} \quad u_{\min} \leq -\mu_1 - \frac{\xi \mu_2 v_{\max}}{\mu_1}. \tag{40}$$

Proof. First consider the case $a > -\mu_1$. As $\alpha_3\big(h_3(\mathbf{x})\big) \geq 0$ for all $\mathbf{x} \in \mathcal{S}_3$, $\mu_1, \mu_2, \xi > 0$, $v_{\max} \geq v \geq 0$, and $v_{\mathrm{L}} \geq 0$, $k_3^{\mathrm{s}}(\mathbf{x})$ in (39) satisfies:

$$k_3^{\mathrm{s}}(\mathbf{x}) \geq a - \frac{\xi \mu_2 v}{\mu_1} > -\mu_1 - \frac{\xi \mu_2 v_{\max}}{\mu_1} \geq u_{\min}. \tag{41}$$

Moreover, since $k_{\mathrm{d}}(\mathbf{x}) \in [u_{\min}, u_{\max}]$, (3), (4), (38), (40) yield $k_3(\mathbf{x}) = \min\{k_{\mathrm{d}}(\mathbf{x}), k_3^{\mathrm{s}}(\mathbf{x})\} \in [u_{\min}, u_{\max}]$.

Next, for $a = -\mu_1$, $k_3(\mathbf{x}) = k_{\mathrm{d}}(\mathbf{x}) \in [u_{\min}, u_{\max}]$.

Finally, for $a < -\mu_1$, $k_3^{\mathrm{s}}(\mathbf{x})$ in (39) satisfies:

$$k_3^{\mathrm{s}}(\mathbf{x}) \leq a < -\mu_1 \leq u_{\max}. \tag{42}$$

Since $k_{\mathrm{d}}(\mathbf{x}) \in [u_{\min}, u_{\max}]$, (3), (4), (38), (40) yield $k_3(\mathbf{x}) = \max\{k_{\mathrm{d}}(\mathbf{x}), k_3^{\mathrm{s}}(\mathbf{x})\} \in [u_{\min}, u_{\max}]$, and Theorem 5 holds. □

Theorem 5 demonstrates that a safety-critical CCC satisfying input constraints can be achieved by properly selecting μ_1 and μ_2. The term $(\xi \mu_2 v_{\max})/\mu_1$ in (40) represents the additional control effort compared to the lag-free case. As the CAV's maximum deceleration $u_{\min}$ is fixed by its braking capability, an increase in ξ necessitates a decrease in μ_1 and μ_2, resulting in a more conservative safe set. Moreover, ensuring input feasibility for $a < -\mu_1$ requires $u_{\max} \geq -\mu_1$, which is typically satisfied as CAVs have $u_{\max} > 0$.

Apart from the control input $k_3(\mathbf{x})$, the CAV's actual acceleration a can also be bounded under certain conditions, leading to increased driving comfort. Consider:

$$h_a(\mathbf{x}) = a + \mu_1, \tag{43}$$

and the corresponding set:

$$\mathcal{S}_a = \{\mathbf{x} \in \mathbb{R}^3 : h_a(\mathbf{x}) \geq 0\}. \tag{44}$$

Corollary 1. *If $k_{\mathrm{d}}(\mathbf{x}) \geq -\mu_1$ holds when $a = -\mu_1$, then system (34) with controller $k_3(\mathbf{x})$ in (3), (38), (39) is safe w.r.t. $\mathcal{S}_a$, that is, $a(t) \geq -\mu_1$ holds for all $t \geq 0$ if $a(0) \geq -\mu_1$.*

Proof. For $h_a(\mathbf{x})$ in (43), we have $\nabla h_a(\mathbf{x}) = \begin{bmatrix} 0 & 0 & 1 \end{bmatrix} \neq \mathbf{0}$. Based on Theorem 1, (34) is safe w.r.t. $\mathcal{S}_a$ if and only if:

$$\dot{h}_a\big(\mathbf{x}, k_3(\mathbf{x})\big) = \frac{k_3(\mathbf{x}) - a}{\xi} \geq 0, \quad \text{when } a = -\mu_1. \tag{45}$$

Based on (38), $k_3(\mathbf{x}) = k_{\mathrm{d}}(\mathbf{x})$ when $a = -\mu_1$. Thus, if $k_{\mathrm{d}}(\mathbf{x}) \geq -\mu_1$ at $a = -\mu_1$, then (45) holds and Corollary 1 applies. □

Corollary 1 shows that, under certain assumptions on the initial condition and nominal controller $k_{\mathrm{d}}(\mathbf{x})$, the CAV's acceleration satisfies $a(t) \geq -\mu_1$. This allows balancing driving comfort and conservativeness by adjusting μ_1: a smaller μ_1 improves comfort, i.e., provides lower deceleration, but shrinks the safe set.

To examine the impact of lag on safety-critical CCC (3), (38), (39), we simulate the same scenario as in Fig. 3 with lag $\xi = 0.6\,\mathrm{s}$; see Fig. 5. We choose μ_1 and μ_2 such that (40) holds, and use the parameters in Table I. Particularly, we enforce $k_{\mathrm{d}}(\mathbf{x}) \in [-\mu_1, u_{\max}]$ to satisfy the conditions in Corollary 1 by substituting $u_{\min}$ with $-\mu_1$ in (4). In Fig. 5(a,b), the CAV's delayed response to the CHV's

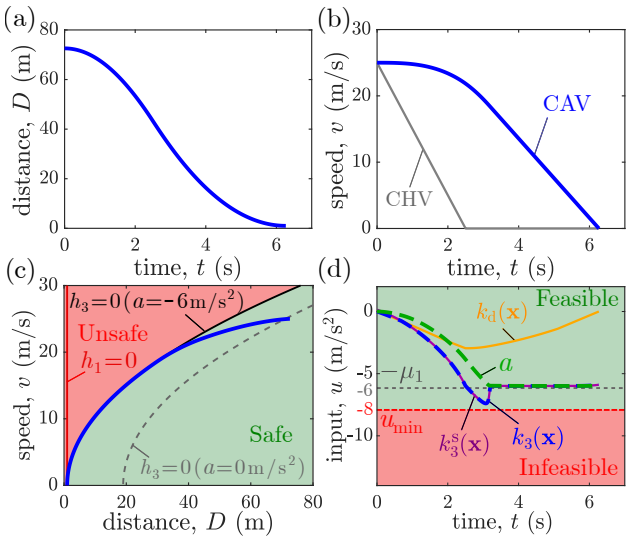

Fig. 5. Simulations of system (2) with $\xi = 0.6$ s using the safety filter with backstepping CBF (3,38,39). Simulations are terminated when $v = 0$.

deceleration leads to a higher velocity and rapidly shrinking distance compared to Fig. 3(a,b). However, the safety filter successfully ensures safety by keeping the state trajectory (blue) within the safe set; see Fig. 5(c). Importantly, the proposed safety-critical CCC can guarantee safety while meeting input constraints; see the input $k_3(\mathbf{x})$ (blue) in Fig. 5(d). Moreover, the CAV's acceleration a (green) in Fig. 5(d) is always larger than $-\mu_1$, as stated by Corollary 1. This implies that selecting a smaller $-\mu_1$ leads to a smaller deceleration magnitude, thus improving driving comfort while maintaining safety. However, this also comes at the cost of a smaller safe region, i.e., increased safe distances. Overall, despite added conservativeness from lag, the proposed safety-critical CCC reliably ensures safety and input constraint compliance, providing a feasible solution for safe operation at all times.

V. Conclusion

This paper proposed a safety-critical connected cruise control (CCC) strategy for connected automated vehicles (CAVs) using backstepping control barrier functions (CBFs). The controller guarantees feasibility and safety, even with first-order lag, by appropriately tuning the backstepping CBF parameters. Analysis revealed that reduced braking capacity, stricter comfort requirements, and increased lag result in a more conservative safe region. Simulations validated the proposed controller on CAVs and demonstrated safety assurance with feasible behavior and comfort. Future work will include a comparison of this framework with other reachability-based feasible CBF approaches.

References

[1] A. Alan, C. R. He, T. G. Molnár, J. C. Mathew, A. H. Bell, and G. Orosz, "Integrating safety with performance in connected automated truck control: Experimental validation," *IEEE Transactions on Intelligent Vehicles*, vol. 9, no. 1, pp. 3075–3088, 2024.

[2] Y. Zheng, J. Wang, and K. Li, "Smoothing traffic flow via control of autonomous vehicles," *IEEE Internet of Things Journal*, vol. 7, no. 5, pp. 3882–3896, 2020.

[3] T. G. Molnár and G. Orosz, "Destroying phantom jams with connectivity and automation: Nonlinear dynamics and control of mixed traffic," *Transportation Science*, vol. 58, no. 6, pp. 1319–1334, 2024.

[4] S. Vaskov, U. Sharma, S. Kousik, M. Johnson-Roberson, and R. Vasudevan, "Guaranteed safe reachability-based trajectory design for a high-fidelity model of an autonomous passenger vehicle," in *American Control Conference*, 2019, pp. 705–710.

[5] L. Wen, J. Duan, S. E. Li, S. Xu, and H. Peng, "Safe reinforcement learning for autonomous vehicles through parallel constrained policy optimization," in *23rd IEEE International Conference on Intelligent Transportation Systems*, 2020, pp. 1–7.

[6] P. Hang, X. Xia, G. Chen, and X. Chen, "Active safety control of automated electric vehicles at driving limits: A tube-based MPC approach," *IEEE Transactions on Transportation Electrification*, vol. 8, no. 1, pp. 1338–1349, 2021.

[7] A. Alan, A. J. Taylor, C. R. He, A. D. Ames, and G. Orosz, "Control barrier functions and input-to-state safety with application to automated vehicles," *IEEE Transactions on Control Systems Technology*, vol. 31, no. 6, pp. 2744–2759, 2023.

[8] Q. Nguyen and K. Sreenath, "Exponential Control Barrier Functions for enforcing high relative-degree safety-critical constraints," in *American Control Conference*, 2016, pp. 322–328.

[9] W. Xiao and C. Belta, "Control barrier functions for systems with high relative degree," in *58th IEEE Conference on Decision and Control*, 2019, pp. 474–479.

[10] A. J. Taylor, P. Ong, T. G. Molnar, and A. D. Ames, "Safe backstepping with control barrier functions," in *61st IEEE Conference on Decision and Control*, 2022, pp. 5775–5782.

[11] T. G. Molnar, A. K. Kiss, A. D. Ames, and G. Orosz, "Safety-critical control with input delay in dynamic environment," *IEEE Transactions on Control Systems Technology*, vol. 31, no. 4, pp. 1507–1520, 2022.

[12] Y. Chen, M. Jankovic, M. Santillo, and A. D. Ames, "Backup control barrier functions: Formulation and comparative study," in *60th IEEE Conference on Decision and Control*, 2021, pp. 6835–6841.

[13] C. R. He and G. Orosz, "Safety guaranteed connected cruise control," in *21st IEEE International Conference on Intelligent Transportation Systems*, 2018, pp. 549–554.

[14] T. G. Molnar, G. Orosz, and A. D. Ames, "On the safety of connected cruise control: Analysis and synthesis with control barrier functions," in *62nd IEEE Conference on Decision and Control*, 2023, pp. 1106–1111.

[15] Y. Chen, T. G. Molnar, and G. Orosz, "Safety-critical connected cruise control: Leveraging connectivity for safe and efficient longitudinal control of automated vehicles," in *27th IEEE International Conference on Intelligent Transportation Systems*, 2024, pp. 110–115.

[16] Y. Chen, G. Orosz, and T. G. Molnar, "Safe and stable connected cruise control for connected automated vehicles with response lag," *arXiv preprint arXiv:2409.06884*, 2024.

[17] J. I. Ge, S. S. Avedisov, C. R. He, W. B. Qin, M. Sadeghpour, and G. Orosz, "Experimental validation of connected automated vehicle design among human-driven vehicles," *Transportation Research Part C*, vol. 91, pp. 335–352, 2018.

[18] L. Zhang and G. Orosz, "Motif-based design for connected vehicle systems in presence of heterogeneous connectivity structures and time delays," *IEEE Transactions on Intelligent Transportation Systems*, vol. 17, no. 6, pp. 1638–1651, 2016.

[19] M. Nagumo, "Über die lage der integralkurven gewöhnlicher differentialgleichungen," *Proceedings of the Physico-Mathematical Society of Japan. 3rd Series*, vol. 24, pp. 551–559, 1942.

[20] A. D. Ames, X. Xu, J. W. Grizzle, and P. Tabuada, "Control barrier function based quadratic programs for safety critical systems," *IEEE Transactions on Automatic Control*, vol. 62, no. 8, pp. 3861–3876, 2017.

[21] M. Jankovic, "Robust control barrier functions for constrained stabilization of nonlinear systems," *Automatica*, vol. 96, pp. 359–367, 2018.

[22] M. Cohen and C. Belta, *Adaptive and Learning-Based Control of Safety-Critical Systems*. Springer, 2023.

[23] X. Tan, W. S. Cortez, and D. V. Dimarogonas, "High-order barrier functions: Robustness, safety, and performance-critical control," *IEEE Transactions on Automatic Control*, vol. 67, no. 6, pp. 3021–3028, 2022.

[24] M. H. Cohen, T. G. Molnar, and A. D. Ames, "Safety-critical control for autonomous systems: Control barrier functions via reduced-order models," *Annual Reviews in Control*, vol. 57, p. 100947, 2024.